Supplemental Material

Supplemental Methods

Supplemental Figures and Figure Legends

Supplemental Table S1: Replication Origins

Supplemental Table S2: ARS consensus sequences

Supplemental Table S3: Yeast strains

Supplemental Table S4: Replication Timing (RT) of all lagging and leading gene copies for WT and *mcm2-3A* strains

Supplemental Table S5: Average DNA synthesis rates of all lagging and leading gene copies for WT and *mcm2-3A* strains

Supplemental_Code.tar

Supplemental Methods

Yeast Strains

All yeast strains have a W303 background and are listed in Supplemental Table S3. The WT strain (RZ71) containing the HA tagged Rpb3 RNAPII subunit was obtained from a cross between ES3086 (courtesy of E. Schwob) and YMTK2567 (courtesy of T. Lee). The *rtt109Δ* strains RZ72 (Figure 4) and RZ23 (Supplemental Fig S5) were obtained by crossing RZ71 with ZGY929 (courtesy of Z. Zhang) and ES3086 and ZGY954 (courtesy of Z. Zhang), respectively. The *rtt109Δ* (RZ72 and RZ23) and *hst3, 4ΔΔ* (PKY4220, courtesy of P. Kaufman, Supplemental Fig S5) strains have been validated by anti H3K56ac western blotting of bulk mid-log cell extracts (Supplemental Fig S13). The *mcm2-3A* strain (AC38) (Figure 6, Supplemental Fig S9, Supplemental Fig S10 and Supplemental Fig S11) was derived from a cross between strains 8566 (courtesy of K. Labib) and RZ71.

Cell Culture

H3K56ac ChIP-NChAP (Figure 3): Cells were grown overnight at 30°C in 500ml Synthetic Complete- URA + Dextrose (SCD-URA) media to OD 0.3. After 3.75hrs at 30°C with α factor (0.15µg/ml), cells were pelleted and transferred into preheated and premixed SCD-URA+ 10µM EdU (Carbosynth), with freshly added 20µg/ml pronase (Sigma). The culture was fixed with 1% formaldehyde after 24min (early S) or 30min (mid S) incubation at 30°C, incubated for 30min at 30°C and quenched with 125mM Glycine. Cell pellets were then washed with water and flash frozen in liquid nitrogen and kept at -80°C until further processing.

Rpb3-HA and H3K56ac ChIP-NChAP (Figs 1, 2, 4, Supplemental Figs S1, S2, S3 and S4):

Cells were grown overnight at 30°C in SCD-URA. The culture was diluted to OD_{600} ~0.3 the next morning and grown to OD_{600} ~0.65 and re-diluted to OD_{600} ~0.3 (total final volume 10 L) in fresh media. The culture was synchronized with the addition of 0.15 µg/ml α factor for 3h30min at 30°C (G1 time points from Figure 2A). Cells were released from arrest as above in preheated (SCD-URA) + 10 µM EdU. At 20, 22, 24, 25, or 32 min after release, cells (2.5 L per time point) were fixed with 1% (w/v) formaldehyde for 15 min at 30°C followed by 5 min of quenching in 125 mM Glycine. Cell pellets were then washed with cold PBS and flash frozen in liquid nitrogen and kept at -80°C until further processing.

Rpb3-HA, H3, H3K4me3, H3K36me3 and H3K56ac ChIP-NChAP (Figs 5, 6, Supplemental Figs S6, S7, S8, and S9):

WT or Mcm2-3A cells were grown and synchronized as above. 3 L culture aliquots were then fixed at 20 and 25 min after release from G1 arrest as above.

WT and Mcm2-3A NChAP time course for replication timing (Supplemental Fig S10):

As above except that cells from 200 ml aliquots were fixed at 18, 25, 32, 40, 48 and 55 min after release from G1 arrest.

Rpb3-HA ChIP-NChAP, EdU-Thymidine pulse chase in asynchronous cultures(Figure S3B):

Mid-log cells (grown o/n in SCD-URA at 30°C, OD_{600} ~0.68) were treated with 10μM EdU for 1min by mixing equal volumes of culture and preheated (30°C) premixed media containing 20μM EdU. EdU incorporation was stopped with the addition of Thymidine (Acros Organics , previously mixed into preheated SCD-URA media) to a final concentration of 10mM (1000 fold excess) to the culture. The culture was divided into two flasks and the ½ cultures were fixed with formaldehyde 7 or 15 minutes after EdU addition. Cell pellets were washed with cold PBS and flash frozen in liquid nitrogen and kept at -80°C until further processing.

MNase digestion

H3K56ac ChIP-NChAP (Fig 3):700μl 0.5mm glass beads were added to frozen cell pellets (equivalent of 100ml cell cultures OD=0.5 or ~1 billion cells), re-suspended in 700μl cell breaking buffer (20% glycerol 100mM Tris-HCl 7.5). Cells were then spheroplasted by bead beating in the Bullet Blender (Next Advance) for 4x3min at strength 8 in the cold room. Spheroplasts were recovered by puncturing the cap of the tube and spinning into 5ml eppendorf tubes at 1000rpm for 3 min. Cells were then centrifuged 5min at maximum speed in a micro centrifuge and the clear top layer was discarded, each pellet was re suspended in 600ul NP buffer (50mM NaCl, 10mM Tris-HCl pH 7.4, 5mM $MgCl_2$, 1mM $CaCl_2$,0.075% NP-40, 0.5mM sperimidine, 1mM βME).The amount of MNase (Worthington Biochemical) was adjusted to the cell density in each tube in order to obtain 80-90% mononucleosomal sized fragments after 20min incubation at 37°C. The reaction was stopped with 10mM EDTA and used for H3K56ac ChIP as described below.

Chromatin Sonication

Cross-linked frozen cell pellets were re-suspended in 1.5 ml NP lysis buffer (100 mM NaCl, 10 mM Tris 7.4, 5 mM MgCl2, 1 mM CaCl2, 10% NP-40, 50 mM EDTA, 0.1 % SDS (optional), 1 mM PMSF and 1xEDTA-free protease inhibitor cocktail (Roche)). The suspension was then split into aliquots each containing ~10^9 cells. Zirconium Sillicate beads (400 μl, 0.5 mm) were then added to each aliquot and cells were mechanically disrupted using a bullet blender (Next Advance)

for 4 times x 3 min (intensity 8). Zirconium beads were removed from the cell lysate by centrifugation and the entire cell lysate was subject to sonication using the Bioruptor-Pico (Diagenode) for 3x10 cycles of 30 seconds *ON/*OFF each, resulting in a final median size of chromatin fragments of 200 bp. Cellular debris was then removed by centrifugation and 2 % of the total supernatant volume was kept for the input and NChAP fractions.

Chromatin Immunoprecipitation (ChIP)

H3K56ac (Figure 3): ChIPs were done as described previously (Radman-Livaja et al. 2010). Antibodies were added to MNase digested chromatin (~10^9 cells/aliquot): 6µl anti- H3K56ac antibody (Merck-Millipore, 07-677-IS (lot# 266732) for the mid-S time point or 10 µl anti- H3K56ac antibody (Active Motif, 39281 (lot# 14013003) for the early-S time point. ChIPed DNA fragments shorter than 100bp were removed with homemade MagNA beads (SeraMag Speed beads, Thermo Scientific,(Rohland and Reich 2012)), and purified fragments were used for NGS library construction (Input, ChIP) or biotin conjugation and subsequent NGS library construction (NChAP, ChIP-NChAP).

Rpb3-HA, H3, H3K4me3, H3K36me3 and H3K56ac (Figs. 1, 2, 4, 5, 6 and Supplemental Figs S1, S2, S3, S4, S6, S7, S8, S9):Sonicated chromatin was precleared using Protein A agarose beads (Repligen) for 1 hour (1h) at 4°C on the rotating wheel. The sonicated material was then pooled together and distributed into 500 µL aliquots (equivalent of 7*10^8 cells per aliquot) and 25 µl of Protein G magnetic beads (Life Technologies-Invitrogen) pre-bound with 6µg, 3µg, 2µg, 4µg, or 3µg of anti-HA (ab9110, abcam) or anti-H3K56ac (Active motif, 39281), anti H3K4me3 (abcam, ab8580), anti H3K36me3 (abcam, ab9050) or anti-H3 (abcam, ab1791) antibodies respectively, was added to each tube. Aliquots were then incubated with rotation at 4°C overnight. The beads were then washed once with cold buffer L (50 mM HEPES-KOH, pH 7.5, 140 mM NaCl, 1 mM EDTA, 1% Triton X-100, 0.1% Na-deoxycholate), three times with cold Buffer W1 (Buffer L with 500mM NaCl), twice with cold Buffer W2 (10 mM Tris-HCl, pH 8.0, 250 mM LiCl, 0.5% NP-40, 0.5% sodium deoxycholate, 1 mM EDTA), and once with cold TE buffer (10 mM Tris-HCl,pH 8.0, 1 mM EDTA). Chromatin was eluted in 2x125 µl elution buffer (25mM Tris-HCl pH 7.5, 5 mM EDTA, 0.5% SDS) after incubation for 2x10 min at 65°C. The eluates and reserved input samples were treated with RNase A (Qiagen) for 1h in 37°C and proteins were then digested with Proteinase K (Euromedex, final concentration 0.4 mg/ml) for 2h at 37°C and the temperature was then shifted to 65°C overnight to reverse cross-links. DNA was then purified with the QIAquick PCR purification kit

(QIAGEN) except for the early S-phase time point (54% unreplicated) from Figs. 1B and 2 that was purified by Phenol Chloroform extraction to keep fragments smaller than 100 bp, which increases the resolution for mapping replication origins. The specificity of H3K56ac antibodies was tested by Western Blot using an H3K56A mutant strain. (Supplemental Fig S13).

Biotin conjugation to EdU with the Click reaction

As described previously in (Vasseur et al. 2016)

Illumina Sequencing Library Construction

ChIP-NChAP and NChAP libraries (Figs 1B, 2, 3, 4, Supplemental Figs S2B, S3 and S4) : As described in (Vasseur et al. 2016).

ChIP-NChAP and NChAP libraries (Figs 5, 6, Supplemental Figs S6, S7, S8, S9, and S10): As above except the TrueSeq V2 LT Sample prep kit (Illumina) was used for the blunt-ending, A tailing and adaptor ligation steps. The primer mix from the kit was also used in the PCR amplification step (15 cycles). All the steps prior to PCR amplification were done with DNA attached to streptavidin beads.

Input and ChIP libraries:

As described in (Vasseur et al. 2016) except libraries for input and ChIP (H3K56ac and Rpb3-HA) fractions from replicates 1 and 2 (52%, 45% and 38% unreplicated) from Fig. S4, for input and Rpb3-HA ChIP from rtt109Δ replicates (17% and 10% unreplicated) from Fig. 4, and for input and all ChIPs in Figs 5, 6, and Supplemental Figs S6, S7, S8 and S9 were prepared using the TrueSeq V2 LT Sample prep kit (Illumina).

The libraries of input fractions from Supplemental Fig S10 were prepared using the NEBNext® Ultra™ II DNA Library Prep Kit for illumina (NEB).

Illumina Sequencing

Libraries were mixed in equimolar amounts (10 to 15 libraries per pool) and library pools were sequenced on a HiSeq 2000 or NovaSeq 6000 (2x75bp) (Illumina) at the CNAG, Barcelona, Spain or the NextSeq550 (2x75bp) (Plateforme Transcriptome, IRMB, Montpellier, France).

RNA-seq with spike-in control (Supplemental Fig S5)

Exponentially growing *S.cerevisiae* (YPD) and *S.pombe* (YES) (strain FY2319, courtesy of S. Forsburg) cells were flash frozen in liquid N2 and total RNA was isolated from frozen cell pellets with TRIzol. Frozen cell pellets were re-suspended directly in TRIzol and bead beated in the Bullet Blender (Next Advance) as above. RNA was then purified and DNAse I treated with the RNAeasy Column purification kit (Qiagen). Extracted total RNA amounts were measured with the

Qubit fluorimeter and the Nanodrop spectrophotometer and the quality was checked by a Bioanalyzer scan (Agilent). Each *S.cerevisiae* total RNA extract was mixed with the *S.pombe* total RNA extract at a mass ratio of 10:1. The mixed RNA samples were then used for NGS library preparation using the Illumina TruSeq Stranded mRNA kit according to the manufacturer's protocol.

ChIP DNA Microarray hybridization (Supplemental Fig S1A)

ChIPed DNA and their corresponding input samples were amplified, with a starting amount of up to 30 ng, using the DNA linear amplification method described previously (Liu et al. 2003; Liu et al. 2005). 2.5 µg of aRNA from each sample produced from the linear amplification was transformed into cDNA by reverse transcription in the presence of amino-allyl dUTP. The resulting cDNA was dye-coupled with Cy5 or Cy3 NHS-esters and purified as described previously (Liu et al. 2005).

Labeled probes (a mixture of Cy5 labeled input and Cy3 labeled ChIPed material or their corresponding dye flips) were hybridized onto an Agilent yeast 4x44 whole genome array (ref. G4810A-14810). Images were scanned at 5µm with the InnoScan 710 MicroArray scanner (Innopsys) and processed with the Mapix software. Data was normalized by dividing the Cy3/Cy5 (or Cy5/Cy3 ratio for the dye flip) ratio for each probe with the average Cy3/Cy5 ratio for the whole array. The average of the pair of normalized ratios from the dye flip technical replicates was used in the final analysis.

Western Blot (Supplemental Fig S13)

Proteins were extracted from whole cells using TCA precipitation according to standard protocols. Protein concentrations were measured by Bradford test kit (Sigma, B6916) and 10 µg/sample was loaded on a 15% polyacrylamide SDS-PAGE gel (30:1 acrylamide/bis-acrylamide). Proteins were transferred to a PDVF membrane (Bio-Rad, 1620177). The membrane was incubated with the anti-H3K56ac antibody (Active motif, 39281) at 1:2000 dilution. We used a secondary goat anti-rabbit-HRP antibody (1:10000, Santa Cruz Biotechnology sc-2054). All antibodies (primary and secondary) were diluted in 5% milk/TBS. We used Immobilon Forte Western HRP substrate (Millipore WBLUF0500) and high-performance chemiluminescent film (Amersham 28906837) for band detection.

Data Analysis

<u>ChIP, ChIP-NChAP, NChAP:</u>

Sequences were aligned to *S.cerevisiae* genome using BLAT (Kent Informatics, http://hgdownload.soe.ucsc.edu/admin/). We kept reads that had at least one uniquely aligned 100% match in the paired end pair. Read count distribution was determined in 1bp windows and then normalized to 1 by dividing each base pair count with the genome-wide average base-pair count. Forward (Watson) and reverse (Crick) reads were treated separately.

The repetitive regions map was constructed by "BLATing" all the possible 70 bp sequences of the yeast genome and parsing all the unique 70bp sequences. All the base coordinates that were not in those unique sequences were considered repetitive.

Normalized read densities for all genes were aligned by the transcription start site (Xu et al. 2009) and median read densities for each coding region (from the tss (not included in the calculation) to the transcription termination site) were determined for all datasets. Median read densities from ChIP and NChAP fractions were normalized to the median from their corresponding input (sonicated or MNase digested chromatin) and medians from ChIP-NChAP fractions were then normalized to the corresponding input normalized ChIP fraction.

The box in the box plot distribution of $\log_2$(lagging/leading) ratios of chromatin feature enrichments is delimited by the lowest (Q_1) and highest (Q_3) value of the second and third quartile, respectively. The line that separates the second and third quartiles represents the median. The right whisker marks either the distribution maximum or (Q_3+1.5*IQR), whichever is smaller (IQR=Q_3-Q_1). The left whisker is either the minimum or (Q_1-1.5*IQR), whichever is higher. Outliers are not shown.

Replicated genome fraction:

Normalized read counts, binned in 400bp windows over the whole genome, from NChAP fractions (and the H3K56ac mid S-phase ChIP fraction since H3K56ac is a mark of new histones that are incorporated into replicated DNA the read density of the H3K56ac ChIP fraction in mid-S-phase mirrors DNA replication, Fig. 3) in each chromosome were divided by the maximum read count for that chromosome to obtain population read densities (i.e. the fraction of the cell population in which each 400bp genome segment has been replicated). We then determined the distribution of these read densities into 100 bins from 1% to 100%. The unreplicated fraction was the genome fraction with read densities between 0 and 1%. For example, in Figure 2, 54% of the genome has a read density of 0 in the early S-phase time point has, i.e. 54% of the genome has not yet been replicated, and ~5% of the genome has a read density of 4, i.e. 4% of the population has replicated 5% of their genome. By early-mid S-phase 50% of cells have replicated at least 0.5% of their genomes and only 10% of the genome has not been replicated in the whole cell population.

Replication origins mapping:

Origins were mapped from the nascent chromatin fraction in the early S-phase datasets from Fig 1B and Fig 2 (54% unreplicated), Fig S8C-D (20min and 25min timepoints) and Fig S10 (18min and 25min timepoints). The resolution between origin centers was higher in these datasets than for origins mapped in (Vasseur et al. 2016) because small fragments (<100bp) were not removed from this fraction (see the Chromatin Immunoprecipitation (ChIP) section). Watson and Crick reads from each dataset were first normalized to input and then normalized to 1 per chromosome by dividing each 10bp segment density with the highest density in the chromosome. We identified local peaks within Replication Origin Associated Domains (ROADS, i.e. replicated regions around known origins of replication, see Figure S11A) on every chromosome (Supplemental Table S1 shows origins identified from the 54% unreplicated dataset from Figures 1B and 2). We then looked for ACS consensus sequences (Nieduszynski et al. 2007) within +-200bp of each identified peak and kept the ACS sequence closest to the peak (Supplemental Table S2). Peaks without ACS sequences were eliminated from further analysis.

Replication timing (Supplemental Fig S10)

Replication timing in Supplemental Fig S10A was determined as described in (Yang et al. 2010). Watson and Crick reads from each time point were first normalized to input and then normalized to 1 per chromosome by dividing each 50bp segment density with the highest density in the chromosome. The normalized densities were then smoothed with a 1600bp moving window average. Read densities for each 50bp segment were then plotted against time. Replication timing was determined from the Hill equation fit : $\%replicated = \frac{1}{1+\left(\frac{t_{50}}{t}\right)^{r}}$, where *t* is the time since release from arrest and the t_{50} is replication timing, i.e. the time since release at which that 50bp segment has been replicated in 50% of the population.

Replication timing values per gene copy from datasets in Figure S10 are listed in Supplemental Table S4.

DNA synthesis rates (Figure 6D and Supplemental Fig S11):

First, replication origins were determined separately for WT and Mcm2-3A strains from NChAP fractions of 18 and 25min time points as above (Supplemental Fig S10). Local peaks were found in read density profiles binned in 50bp windows and normalized as above for replication timing calculations. Second, genes that are replicated from each origin were grouped into Replication Origin Associated Domains (ROADs) from Watson and Crick strands

in both time points. The average DNA synthesis rates of the Watson and Crick strands at each gene from every ROAD were calculated from the slope of the linear fit of the gene coordinates in bp versus replication timing. Synthesis rates of lagging strand gene copies are derived from slopes from the Watson strand upstream of origins and the Crick strand downstream of origins. Conversely leading strand synthesis rates come from Crick strands upstream and Watson strands downstream of origins.

DNA synthesis rates per gene copy from Fig 6D using ROADs determined from datasets in Fig S10 and S11 are listed in Supplemental Table S5.

The Perl scripts used for origin mapping and to calculate replication timing and DNA synthesis rates are provided in the Supplemental_Code.tar file.

RNA-seq normalized to *S.pombe* spike-in (Supplemental Fig S5):

S.cerevisiae and *S.pombe* reads were aligned to their respective genomes using BLAT and the read density distribution was determined for each species in each dataset separately. The average S.pombe genomic read density per bp (F and R reads were processed together) was determined for each dataset. For spike-in normalization, *S.cerevisiae* read densities per bp were then divided with the corresponding *S.pombe* average genomic read density. For internal normalization *S.cerevisiae* read densities were divided with its average genomic read density as described above. Normalized read densities for each gene were aligned by the transcription start site and divided into sense and antisense transcripts. The median read density for each gene (from the tss to the end of the coding sequence) was then determined for each transcript. Intron regions were excluded from the calculation.

Liu CL, Kaplan T, Kim M, Buratowski S, Schreiber SL, Friedman N, Rando OJ. 2005. Single-nucleosome mapping of histone modifications in S. cerevisiae. *PLoS Biol* **3**: e328.

Liu CL, Schreiber SL, Bernstein BE. 2003. Development and validation of a T7 based linear amplification for genomic DNA. *BMC Genomics* **4**: 19.

Nieduszynski CA, Hiraga S, Ak P, Benham CJ, Donaldson AD. 2007. OriDB: a DNA replication origin database. *Nucleic Acids Res* **35**: D40-46.

Radman-Livaja M, Liu CL, Friedman N, Schreiber SL, Rando OJ. 2010. Replication and active demethylation represent partially overlapping mechanisms for erasure of H3K4me3 in budding yeast. *PLoS Genet* **6**: e1000837.

Rohland N, Reich D. 2012. Cost-effective, high-throughput DNA sequencing libraries for multiplexed target capture. *Genome Res* **22**: 939-946.

Vasseur P, Tonazzini S, Ziane R, Camasses A, Rando OJ, Radman-Livaja M. 2016. Dynamics of Nucleosome Positioning Maturation following Genomic Replication. *Cell Reports* **16**: 2651-2665.

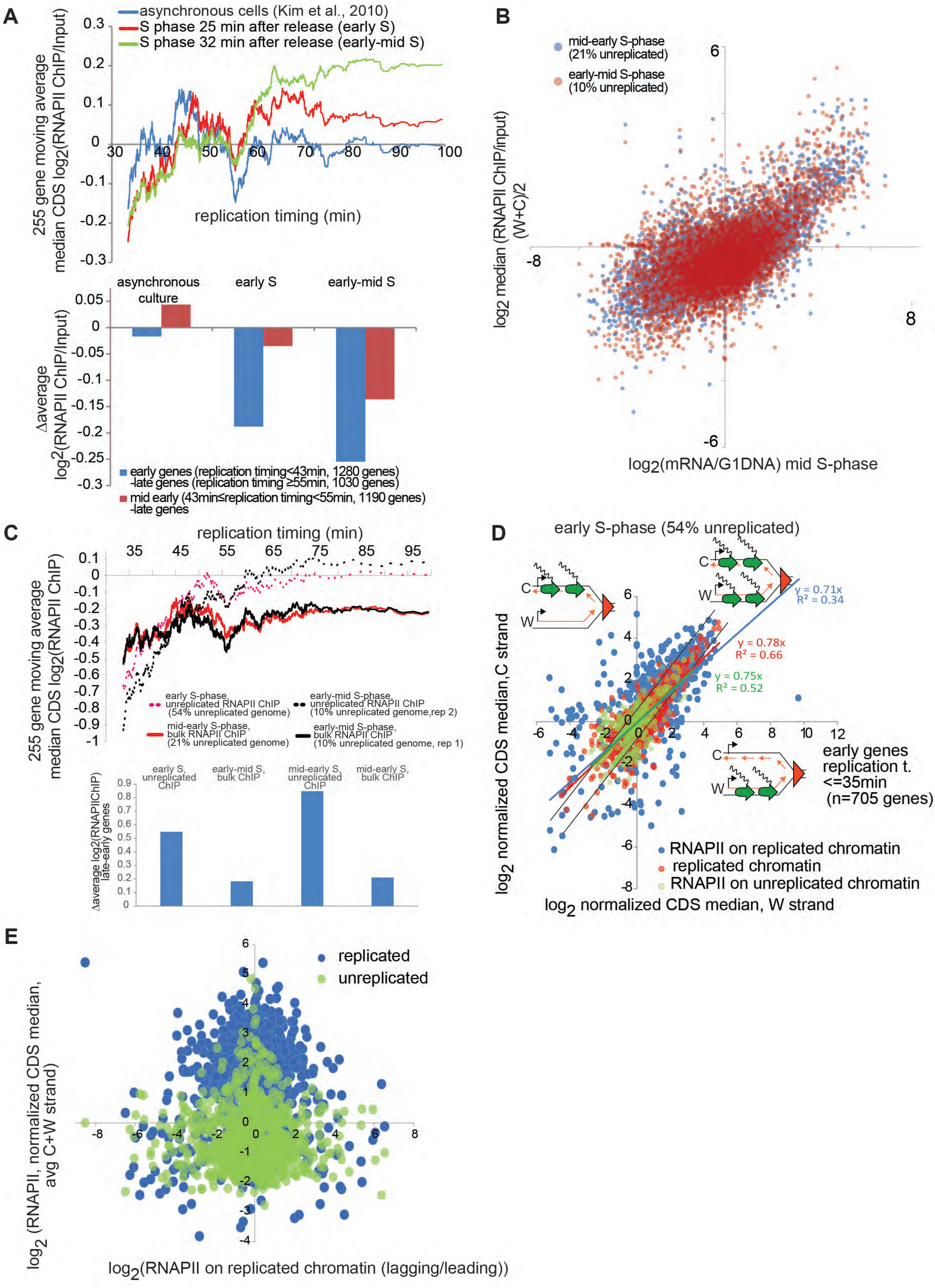

Figure S1: RNAPII is limiting after replication and is distributed more asymmetrically on replicated chromatids at genes with low RNAPII density.

Supplemental Fig S1: RNAPII is limiting after replication and is distributed more asymmetrically on replicated chromatids at genes with low RNAPII density (related to Figures 1 and 2). A. Correlation between the 255 gene moving window average of the median RNAPII occupancy (RNAPII ChIP/DNA input) in the coding sequence of each yeast gene (excluding promoters) and gene replication timing (Vasseur et al., 2016). RNAPII occupancy was measured in synchronized WT cells in early (25min after release from G1 arrest) and early-mid (32min) S-by. DNA isolated by HA tagged RNAPII ChIP and its corresponding input DNA were mixed and hybridized to whole genome two channel microarrays (4×44K Agilent). Occupancy values are an average of two dye flip technical replicates. Bottom: Difference in average $\log_2$ (RNAPII/input) between early and late genes (blue) and mid early and late genes (red) in asynchronous, or in early and mid-early S-phase cultures. Ratio values on the Y axis have been normalized to 0 by subtracting the average $\log_2$(RNAPII/input) for all genes from the $\log_2$(RNAPII/input) for each gene. Release media contained 10mM EdU**. B.** Correlation between bulk RNAPII occupancies in mid-early and early-mid S-phase (replicate 1) and mRNA abundance in mid S-phase. (from the heat map in Figure 2A). **C.** Top: Correlation between the 255 gene moving window average of the median RNAPII occupancy from unreplicated and bulk ChIP fractions (from Figure 2A, RNAPII ChIP) in the coding sequence of each yeast gene (excluding promoters), and gene replication timing (Vasseur et al., 2016). Bottom: Difference in average $\log_2$ (RNAPII ChIP) between late and early genes (as defined in Figure 2A). **D.** Watson (W) versus Crick (C) copies scatter plot of median read densities in coding regions of early replicating genes (**Figure 2A**) for RNAPII on replicated chromatin (ChIP-NChAP fraction, blue), replicated chromatin (NChAP fraction, red), and RNAPII on un-replicated chromatin (ChIP, un-replicated fraction, green). The colors of equations and R^2 for the least square linear fit models of each fraction correspond to the colors of the points in the graph. **E.** Scatter plot of the ratio of RNAPII occupancy between the lagging and the leading gene copy for all 705 early genes from C and the average median RNAPII density (average of W and C copies) on replicated chromatin (blue) and un-replicated chromatin (green). Genes with the largest difference in lagging and leading RNAPII occupancy after replication have low expression and low RNAPII density.

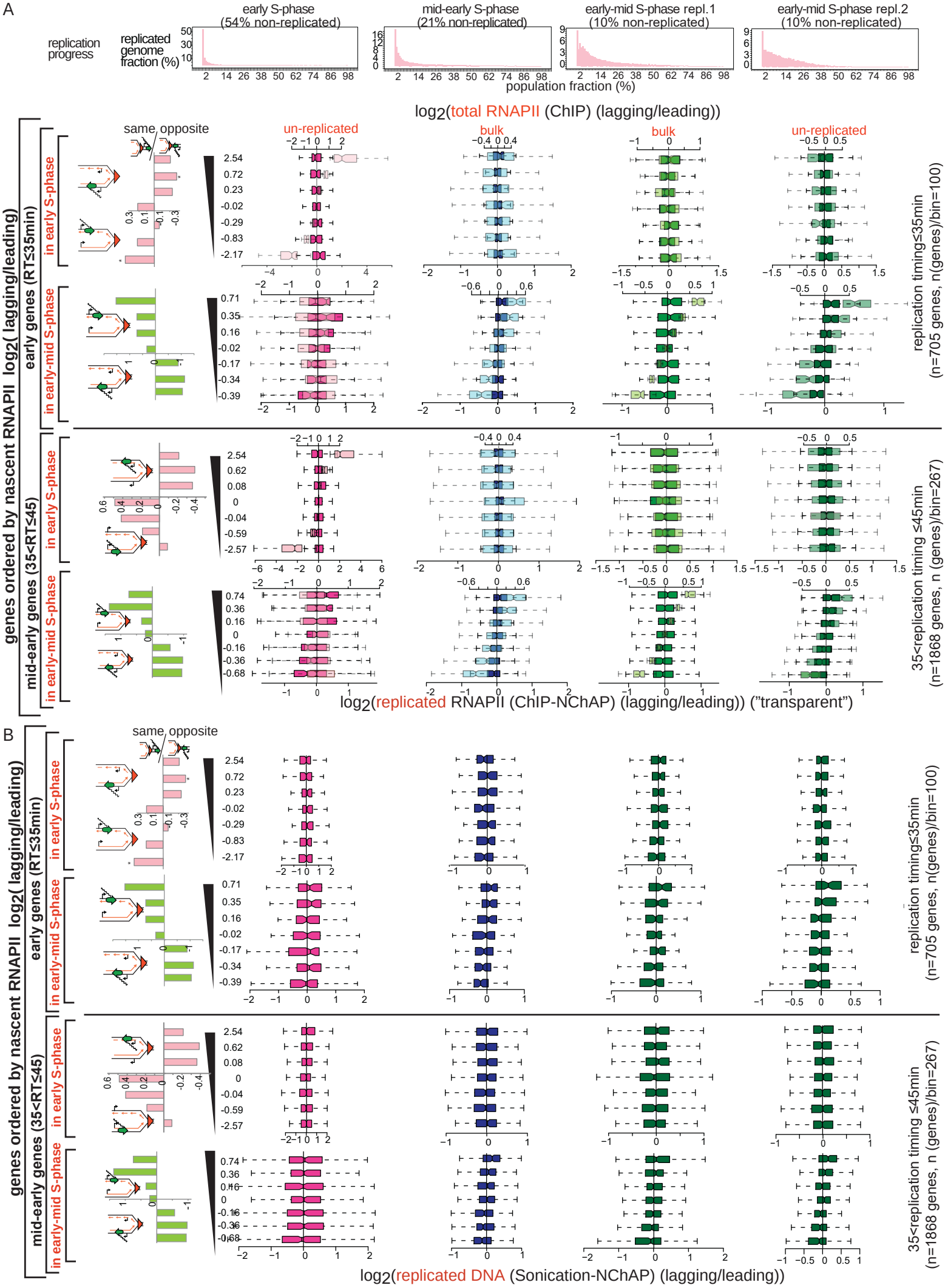

Figure S2: Lagging and Leading strand read density distributions from ChIP (bulk and non-replicated) and NChAP (nascent chromatin) are symmetrical.

Supplemental Fig S2: Lagging and Leading strand read density distributions from ChIP (bulk and un-replicated) and NChAP (replicated chromatin) are symmetrical (related to Figure 2). A. As in Figure 2B with $\log_2$ (total RNAPII (ChIP) (lagging/leading)) box plots in dark superimposed on $\log_2$(replicated RNAPII (ChIP-NChAP)(lagging/leading)) distributions in light/transparent boxes. **B.** $\log_2$(replicated DNA (NChAP)(lagging/leading)) box plot distributions.

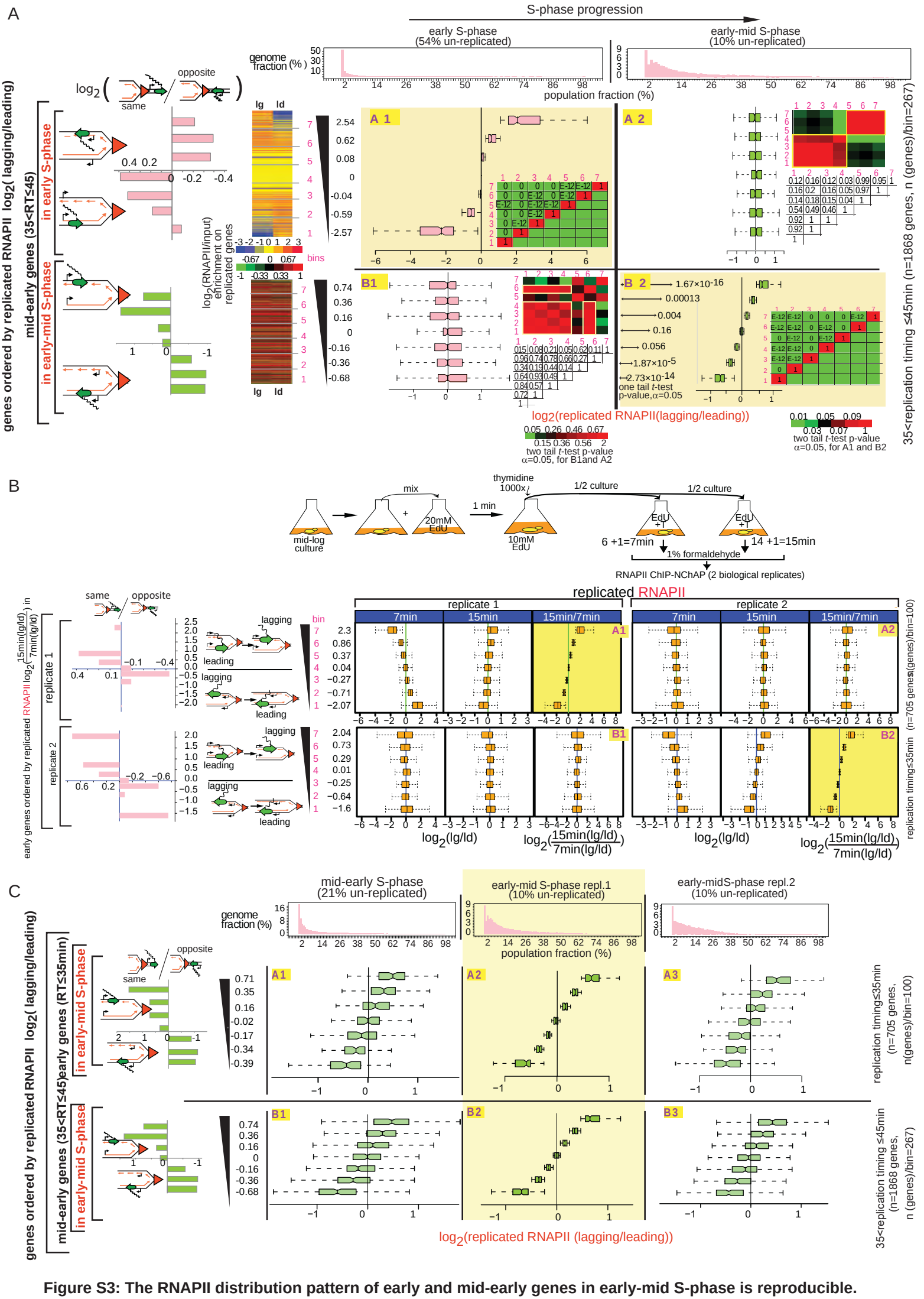

Figure S3: The RNAPII distribution pattern of early and mid-early genes in early-mid S-phase is reproducible.

Supplemental Fig S3: The RNAPII distribution pattern of early and mid-early genes in early-mid S-phase is reproducible (related to Figure 2). A. same as Figure 2B but for mid-early genes. **B.**RNAPII ChIP-NChAP after EdU-Thymidine pulse chase in an asynchronous culture. (Top panel) Experimental outline. (Bottom panel) Box plot distributions of lagging(lg)/leading(ld) RNAPII occupancy 7min and 15min after EdU pulse and Thymidine chase steps. Early genes have been sorted by the decreasing difference in lagging/leading RNAPII occupancy between the 15min and the 7min time points (log2(15min(lg/ld)/7min(lg/ld))) in replicate 1 (row A, yellow panel labeled "15min/7min") and replicate 2 (row B, yellow panel labeled "15min/7min"), divided into 7 bins (y axis), and box plot distributions of replicated RNAPII lagging/leading ratios (x axis) have been determined for each bin for every time point in each replicate as in Figure 2B. The average log2(15min(lg/ld)/7min(lg/ld)) ratios for each bin are shown in the y axis on the left of the box plot panels in each row. As illustrated in the diagrams on the left of the box plot panels, when (log2(15min(lg/ld)/7min(lg/ld)))>0, RNAPII enrichement shifts from the leading copy at the 7min time point to the lagging copy at the 15min time point (bins 5 to7 in fields A1 and B2), and when (log2(15min(lg/ld)/7min(lg/ld)))<0, RNAPII enrichement shifts from the lagging copy at the 7min time point to the leading copy at the 15min time point (bins 1 to3 in fields A1 and B2).The bar graphs on the left show the "same" gene enrichment for gene bins indicated in the Y axis of each row on the right as in Figure 2B. As expected from the results in Figure 2B, transcription mostly travels in the same direction as replication on genes where RNAPII shifts from the leading copy to the lagging copy, while transcription and replication are mostly going in opposite directions on genes where RNAPII shifts from the lagging copy to the leading copy. **C.** Box plot distributions of lagging/leading RNAPII occupancy ratios from mid-early and early-mid S-phase (Figure 2A) for early and mid-early genes (rows A and B, respectively). The header row shows the distribution of genome read densities from the replicated DNA fraction (NChAP) as in Figure 2B. Early and mid-early genes in rows A and B, respectively have been sorted by decreasing lagging/leading RNAPII occupancy in early-mid S-phase (replicate 1, fields A2 and B2, yellow background) and divided into 7 bins (y axis), and box plot distributions of replicated RNAPII lagging/leading ratios (x axis) have been determined for each bin in all three replicates as in Figure 2B. The bar graphs on the left show the "same" gene enrichment for gene bins indicated in the Y axis of each row on the right as in Figure 2B.

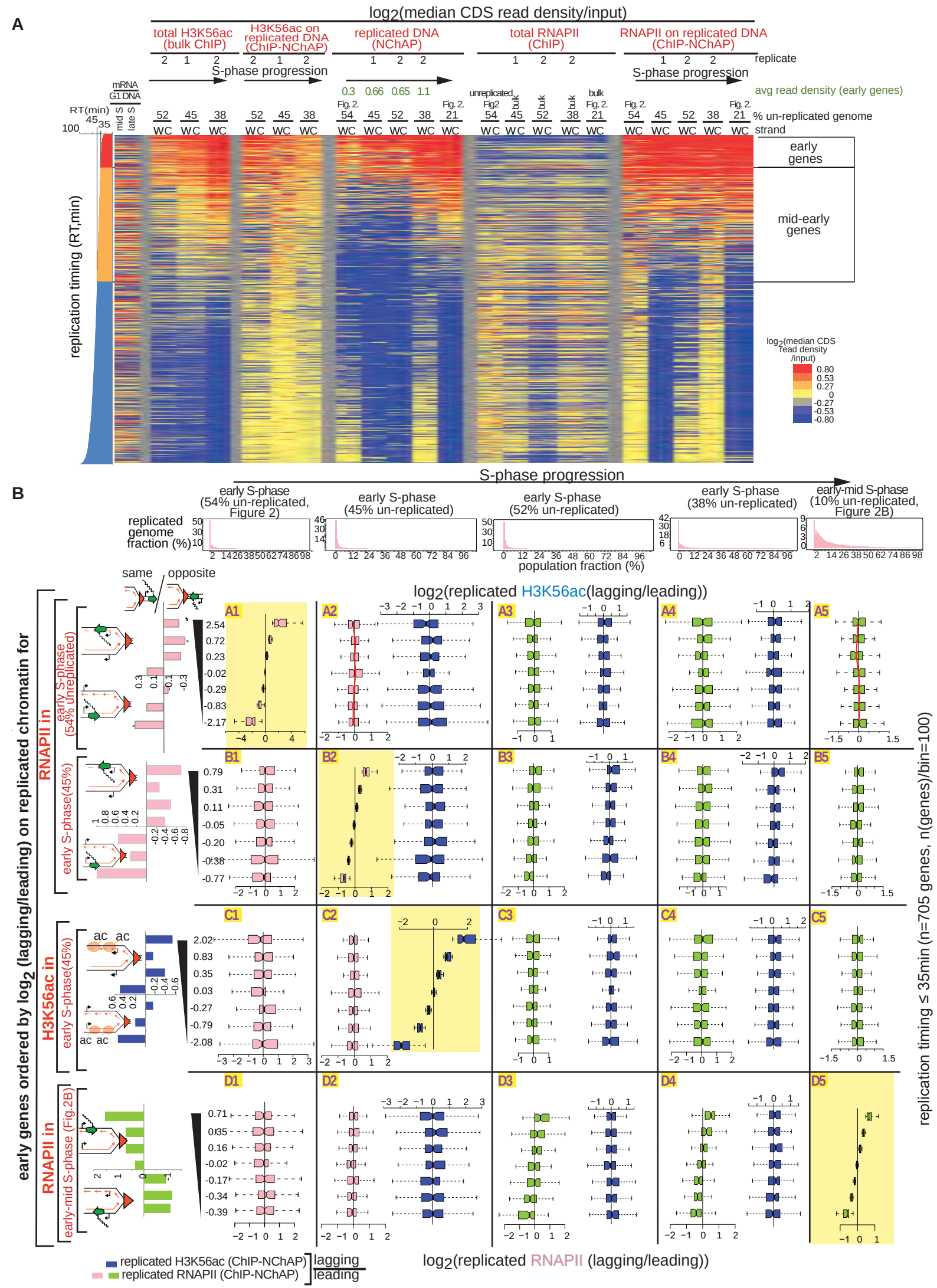

Figure S4: Asymmetric distribution patterns of RNAPII and H3K56ac on replicated gene copies do not correlate:replicate time-course in early S-phase.

Supplemental Fig S4: Asymmetric distribution patterns of RNAPII and H3K56ac on replicated gene copies do not correlate in early S-phase (related to Figure 3). **A.** The heat map shows median RNAPII and H3K56ac occupancies in coding regions (CDS) of all yeast genes that are not regulated by the cell cycle. H3K56ac and RNAPII ChIPs were performed in parallel from the same cell culture as indicated by the label of the biological replicate (1 or 2). Each line is an individual gene and columns represent median read densities for (W)atson and (C)rick gene copies from total H3K56ac or RNAPII (ChIP) and H3K56ac or RNAPII on replicated DNA (ChIP-NChAP) fractions at indicated time points during early S-phase: 45% un-replicated (replicate 1), 52% and 38% un-replicated (replicate 2). Early-mid S-phase (21% un-replicated) and early S-phase (54% un-replicated) datasets from Figure. 2 are added for comparison. The first two columns on the left represent mRNA enrichment over G1 genomic DNA in mid and late S-phase (in the absence of EdU) determined with gene expression microarrays (Vasseur et al., 2016). Genes are ordered by replication timing as in Figure 2 shown in the bar graph on the left (Vasseur et al., 2016). Median read density values for each gene have been normalized as in Figure 2. Due to the stochastic nature of replication origin activation it is impossible to precisely reproduce each early S-phase time point from one biological replicate to the other. Early S-phase time points were therefore further sorted according to replication progress by calculating the average density of the replicated DNA fraction (NChAP) of W and C reads for early genes (n=705), which shows that the replicate from Figure 2 (54% un-replicated) with an average NChAP read density of 0.3 is the earliest time point, followed by the 45% and the 52% un-replicated points, which are at the same stage in S-phase (with 0.66 and 0.65 average read densities, respectively) and finally with the 38% un-replicated time-point as the latest in early S-phase (1.1 average read density of early genes). **B.** Box plot distributions of lagging/leading RNAPII and H3K56ac ratios from early to early-mid S-phase (columns 1 to 5) for early genes. Genes have been organized into bins of increasing lagging/reading ratios (fields with the yellow background) for RNAPII in: early S-phase (dataset from Figure 2; row A), early S-phase (dataset from Supplemental Fig S4A, 45% un-replicated; row B), H3K56ac in early S-phase (45% un-replicated; row C) and early-mid S-phase (from Figure 2, replicate 1; row D). The header row shows the distribution of genome read densities from the replicated DNA fraction (NChAP) as in Figure 2B. The bar graphs on the left show the “same” gene enrichment calculated as in Figure. 2B for gene bins indicated in the Y axis of each row on the right.

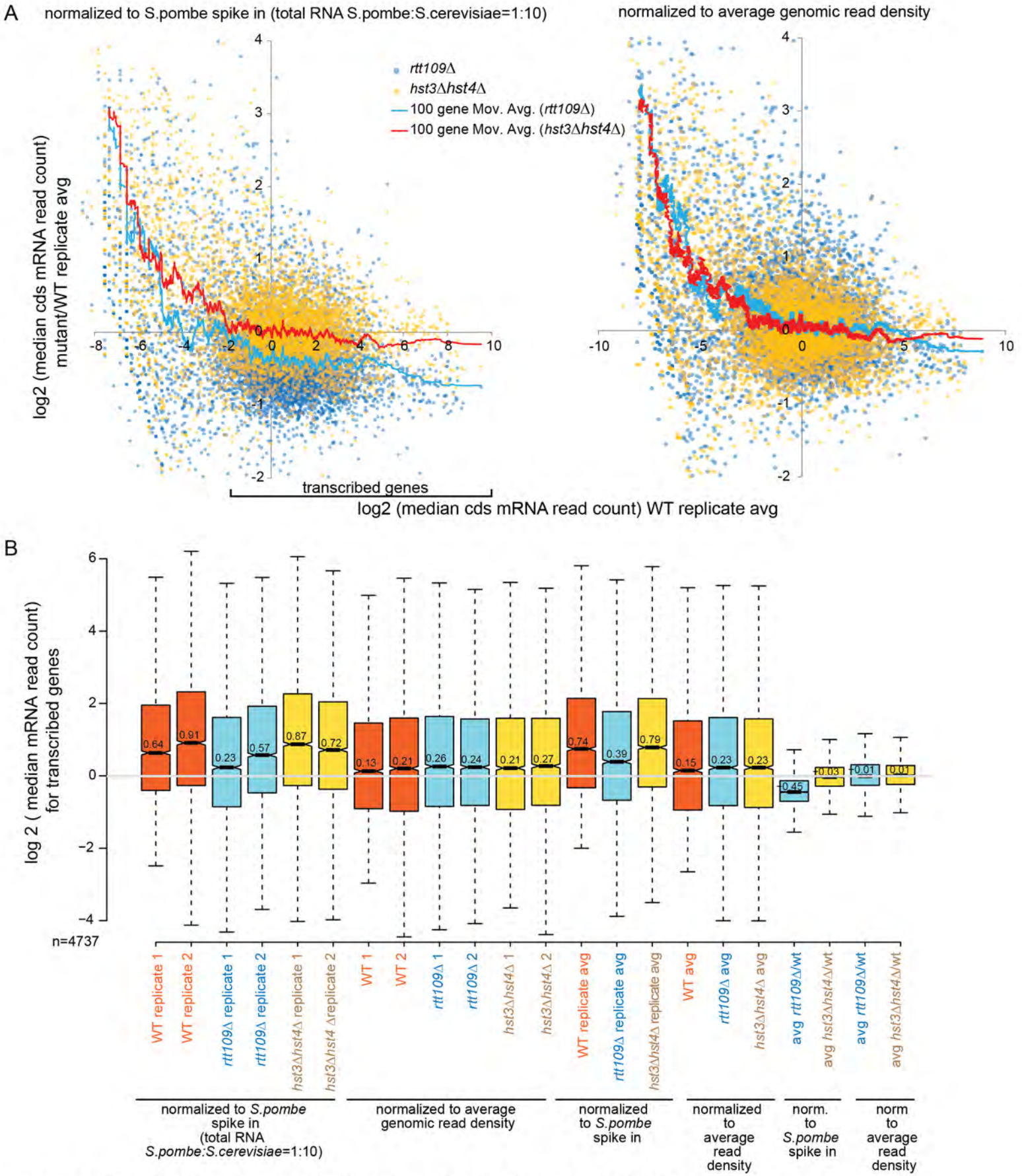

Figure S5: mRNA levels are globally reduced in the absence of H3K56ac.

Supplemental Fig S5: mRNA levels are globally reduced in the absence of H3K56ac (related to Figures 3 and 4). A. Total RNA was isolated from WT, *rtt109Δ* (H3K56 acetylase) and *hst3Δhst4Δ* (H3K56 deacetylases) exponentially growing cells (2 replicates each). Total RNA from *S.pombe* was added to each sample in a 1:10 (cerevisiae to pombe) ratio. Strand specific high-throughput sequencing libraries were then made from isolated polyA RNA. *S.cerevisiae* sequencing reads were normalized to the average genomic read density of the *S.pombe* spike in (left) or of the *S.cerevisiae* sample (right). Median sense mRNA levels for each gene (introns were excluded from the calculation) were determined in all samples. The scatter plots show the ratio between mutant and WT mRNA levels for each gene relative to WT mRNA levels. Spike in normalization (left) reveals that mRNA levels in *rtt109Δ* cells are globally reduced compared to WT, while deletion of *hst3/4* deacetylase genes has no effect on steady state transcription output. Relative gene expression levels are not affected in either mutant as shown with the internally normalized datasets on the right. **B.** Box plot distributions of median mRNA levels per gene coding region for indicated datasets. Only transcribed genes (shown in A (left panel) were used for the analysis (4737 genes). The average median decrease in global mRNA levels in *rtt109Δ* cells relative to WT cells is ~30% ($1-2^{-0.45}$)

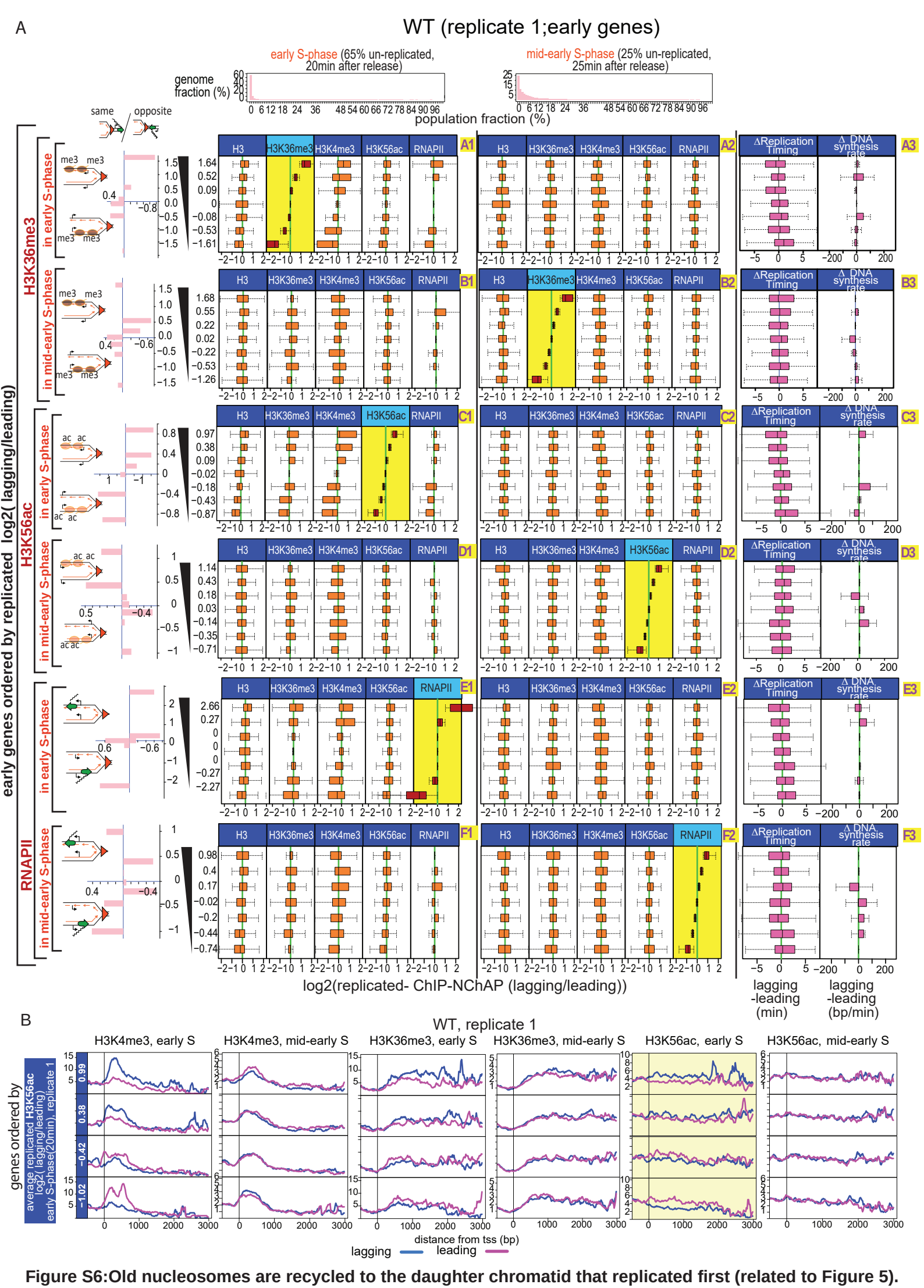

Figure S6:Old nucleosomes are recycled to the daughter chromatid that replicated first (related to Figure 5).

Supplemental Fig S6: Old nucleosomes are recycled to the daughter chromatid that replicated first (related to Figure **5). A.** Box plot distributions of lagging/leading ChIP-NChAP ratios for H3, H3K36me3, H3K4me3, H3K56ac and RNAPII from early and mid-early S-phase for early genes from the same WT culture (biological replicate 1). The histograms in the header show the distribution of genome read densities (in 400bp bins) normalized to the maximum read density for each NChAP (replicated DNA) fraction at indicated time points in S-phase as in Figure 5. Genes have been sorted by decreasing lagging/leading ratios of H3K36me3 in early S-phase (row A) and mid-early S-phase (B), H3K56ac in early S-phase (C) and mid-early S-phase (D), and RNAPII in early S-phase (E) and mid-early S-phase (F), (yellow background), and divided into 7 bins (y axis on the left) as in Figure 5. Box plot distribution of lagging/leading ratios (x axis) for the chromatin features indicated in the headers have been determined for each bin. The bar graphs on the left show the "same" gene enrichment for gene bins indicated in the y axis of each row on the right. Column 3 shows box plot distributions for: the difference in replication timing (ΔRT, left) and DNA synthesis rate (ΔDNA synthesis rate, right) between the lagging and the leading strand for each gene calculated as in Figure 5. **B.** Average tss (transcription start site) centered metagene profiles of ChIP -NChAP fractions indicated in the header from WT cells (replicate 1) from gene bins from A sorted according to the average $\log_2$(lagging/leading) ratios for H3K56ac in early S-phase. Only the two bottom (bins 1-2) and top (bins 6-7) bins are shown. The value of the average ratio for each bin is indicated in the blue strip on the left

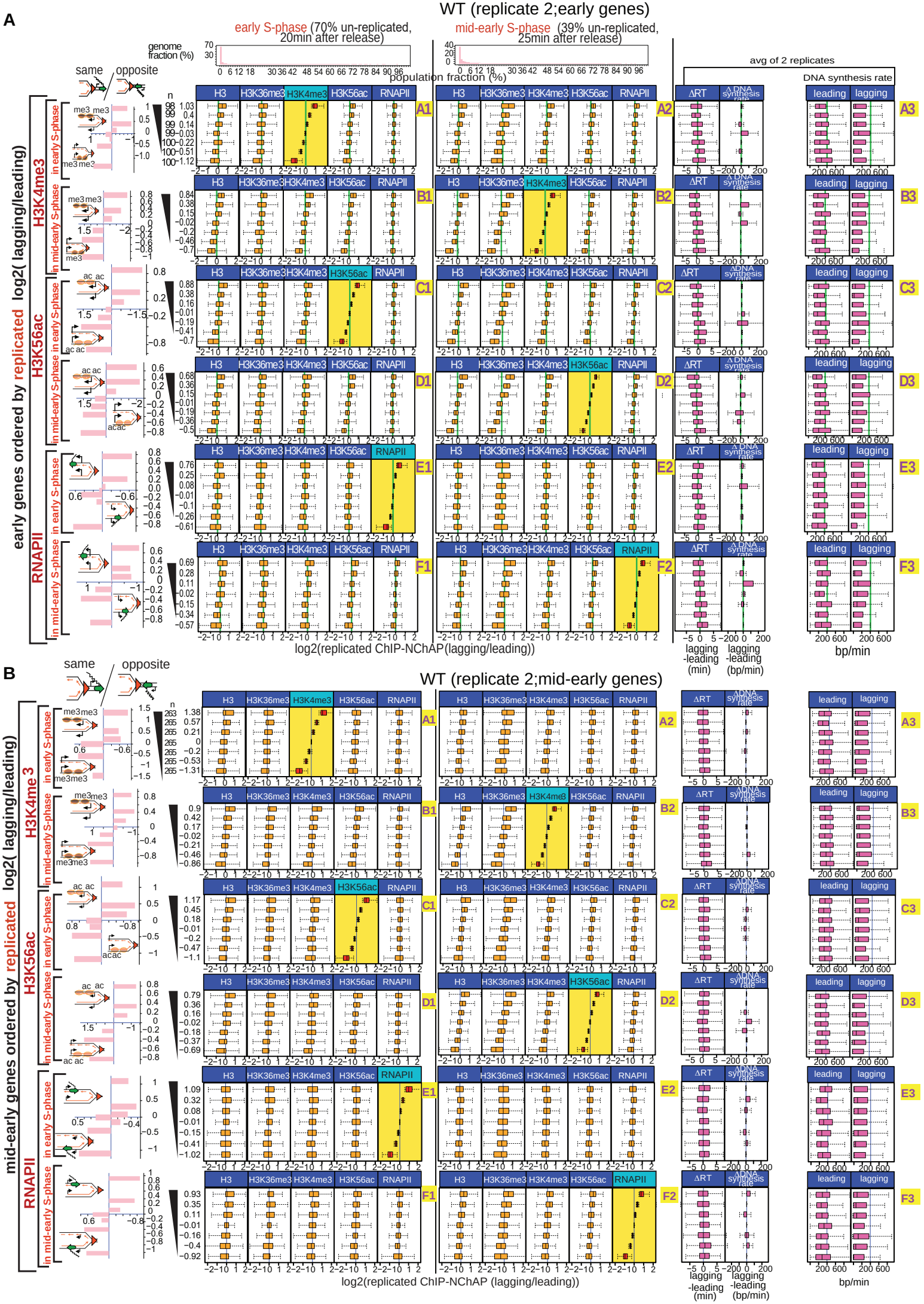
A
WT (replicate 2;early genes)
early S-phase (70% un-replicated, 20min after release)
mid-early S-phase (39% un-replicated, 25min after release)
genome fraction (%)
population fraction (%)
avg of 2 replicates
DNA synthesis rate
same
opposite
n
H3
H3K36me3
H3K4me3
H3K56ac
RNAPII
ΔRT
Δ DNA synthesis rate
leading
lagging
A1
A2
A3
B1
B2
B3
C1
C2
C3
D1
D2
D3
E1
E2
E3
F1
F2
F3
H3K4me3
H3K56ac
RNAPII
in early S-phase
in mid-early S-phase
early genes ordered by replicated log2(lagging/leading)
log2(replicated ChIP-NChAP(lagging/leading))
lagging -leading (min)
lagging -leading (bp/min)
bp/min
B
WT (replicate 2;mid-early genes)
mid-early genes ordered by replicated log2(lagging/leading)
log2(replicated ChIP-NChAP (lagging/leading))

C

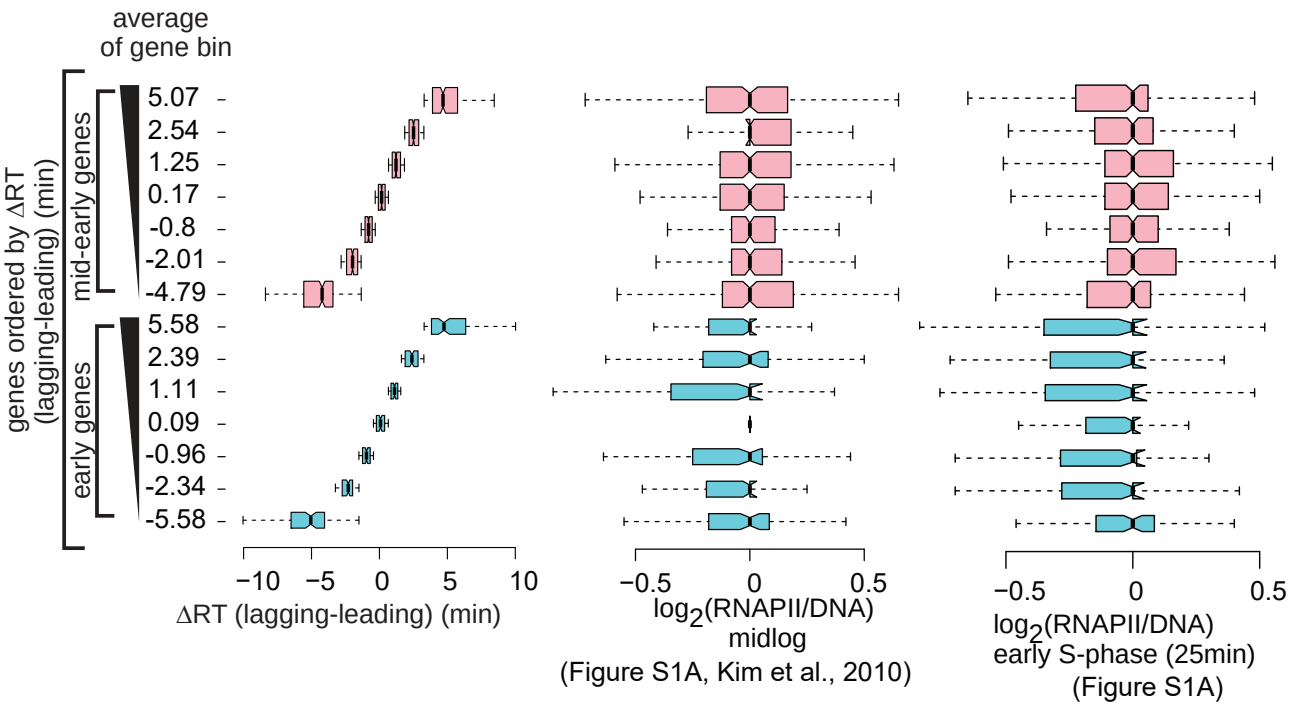

Figure S7: Old nucleosomes are recycled to the daughter chromatid that replicated first and replication timing differences are not linked to transcription levels (related to Figures 5 and S6).

Supplemental Fig S7: Old nucleosomes are recycled to the daughter chromatid that replicated first and replication timing differences are not linked to transcription levels (related to Figure 5 and Supplemental Fig S6). A-B. Box plot distribution of H3, H3K4me3, H3K36me3, H3K56ac and RNAPII on the lagging and leading strand for WT biological replicate 2, for early (A) and mid-early genes (B). The layout is the same as in Figures 5A and Supplemental Fig 6A. **C.** Early and mid-early genes (defined in Figure 2A) have been sorted by the difference in replication timing between the lagging and the leading gene copy (ΔRT) and divided into seven bins (the average ΔRT for each been is shown in the Y axis on the left). Box plot distribution for ΔRT (left), total RNAPII enrichment over DNA content in midlog (middle) and in early S-phase (right) have been determined for each bin. Note that the distribution of RNAPII enrichment in the bins with the highest difference in ΔRT are similar to the distributions in bins with low differences in ΔRT.

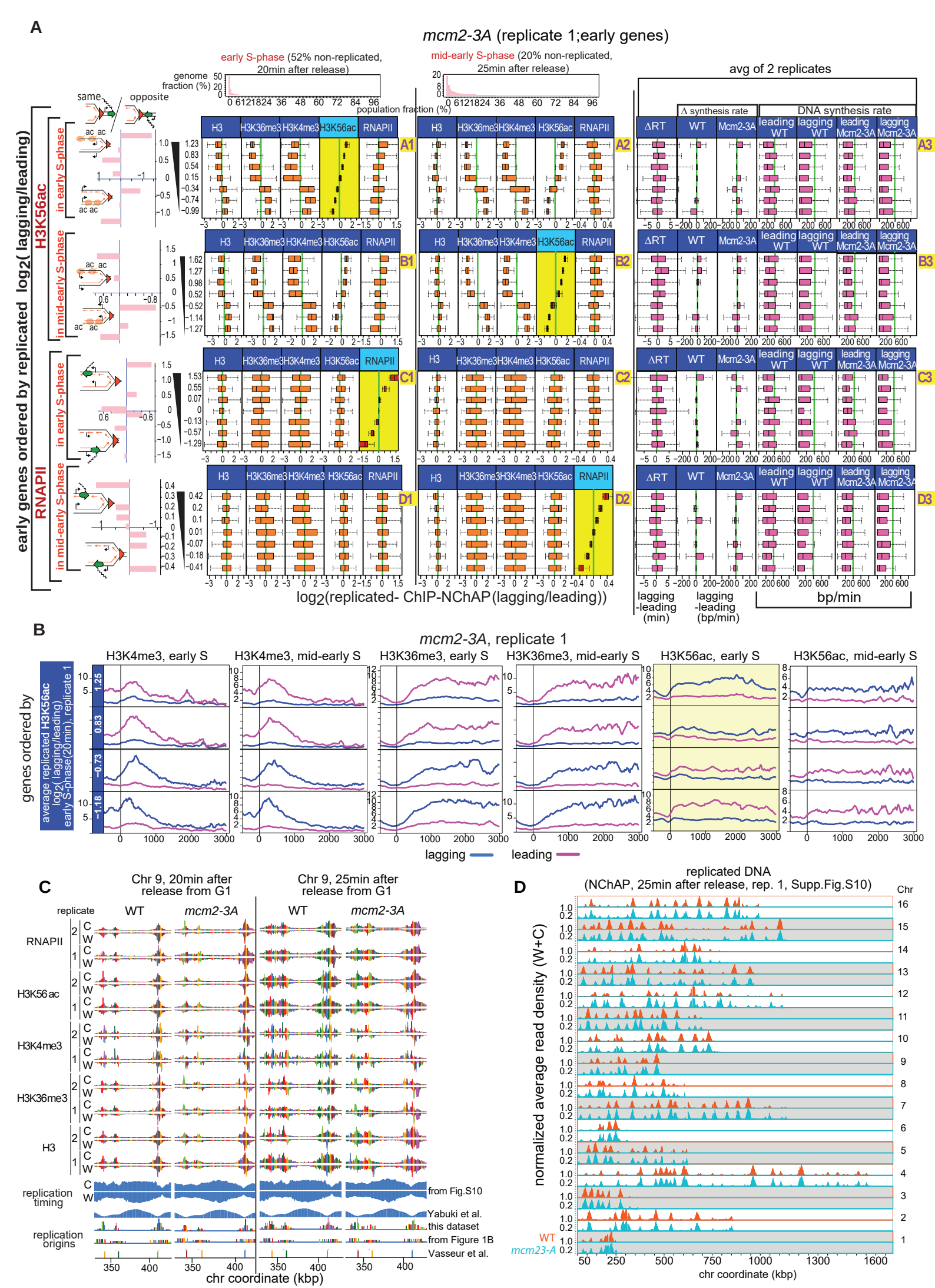

Figure S8:Chromatin maturation in *mcm2-3A* cells (related to Figure 6)

Supplemental Fig S8: Chromatin maturation in *mcm2-3A* cells (related to Figure 6) A. Box plot distributions of lagging/leading ChIP-NChAP ratios for H3, H3K36me3, H3K4me3, H3K56ac and RNAPII from early and mid-early S-phase for early genes measured in the same culture of *mcm2-3A* mutant cells (biological replicate 1). The histograms on top show the distribution of genome read densities (in 400bp bins) normalized to the maximum read density for each NChAP (replicated DNA) fraction at indicated time points in S-phase. Rows A-D: genes have been sorted by decreasing lagging/leading occupancy of H3K56ac in early S-phase (A), H3K56ac in mid-early S-phase (B), RNAPII in early S-phase (C) and RNAPII in mid-early S-phase (D), respectively (yellow background), and divided into 7 bins (y axis on the left). Box plot distribution of lagging/leading ratios (x axis) for the chromatin features indicated in the header have been determined for each bin as in Figure 6A. The bar graphs on the left show the "same" gene enrichment for gene bins indicated in the Y axis of each row on the right. Column 3 shows box plot distributions for, from left to right: the difference in replication timing (ΔRT) between the lagging and the leading strand for each gene in *mcm2-3A* cells; ΔDNA synthesis rate in WT and *mcm2-3A* cells, and average leading and lagging DNA synthesis rates in WT and *mcm2-3A* cells used to obtain the ΔDNA synthesis rates as in Figures 5A and 6A. **B.** Average tss (transcription start site) centered metagene profiles of ChIP -NChAP fractions indicated in the header from *mcm2-3A* mutants (replicate 1) from gene bins sorted according to the average $\log_2$(lagging/leading) ratios for H3K56ac in early S-phase from A. Only the two bottom (bins 1-2) and top (bins 6-7) bins are shown. The value of the average ratio for each bin is indicated in the blue strip on the left. **C**. 400bp binned read density of ChIP-NChAP fractions for RNAP2, H3K56ac, H3K4me3, and H3K36me3 on a segment from Chr 9 measured in two WT and two *mcm2-3A* replicates at 20 (early S) and 25min (mid-early S) after release from alpha factor G1 arrest. Genes are delimited by different colors. The Watson (W) and Crick(C) strands are counted separately. Read densities were first normalized to the genome wide-average read density for each time-point and then each 400bp segment was divided with the highest density in the chromosome to get read densities from 0 to 1. Replication timing profiles in the 6th and 7th row from the bottom are taken from the datasets in Supplemental Fig S10. **D.** 400bp binned read density of NChAP fractions on all chromosomes from WT and *mcm2-3A* cells 25min (mid-early S) after release from alpha factor G1 arrest (the data are from the 25min time point of replicate 1 from the time course in Figure S10). The profiles show an average of Watson (W) and Crick(C) read densities and peaks are centered on replication origins.

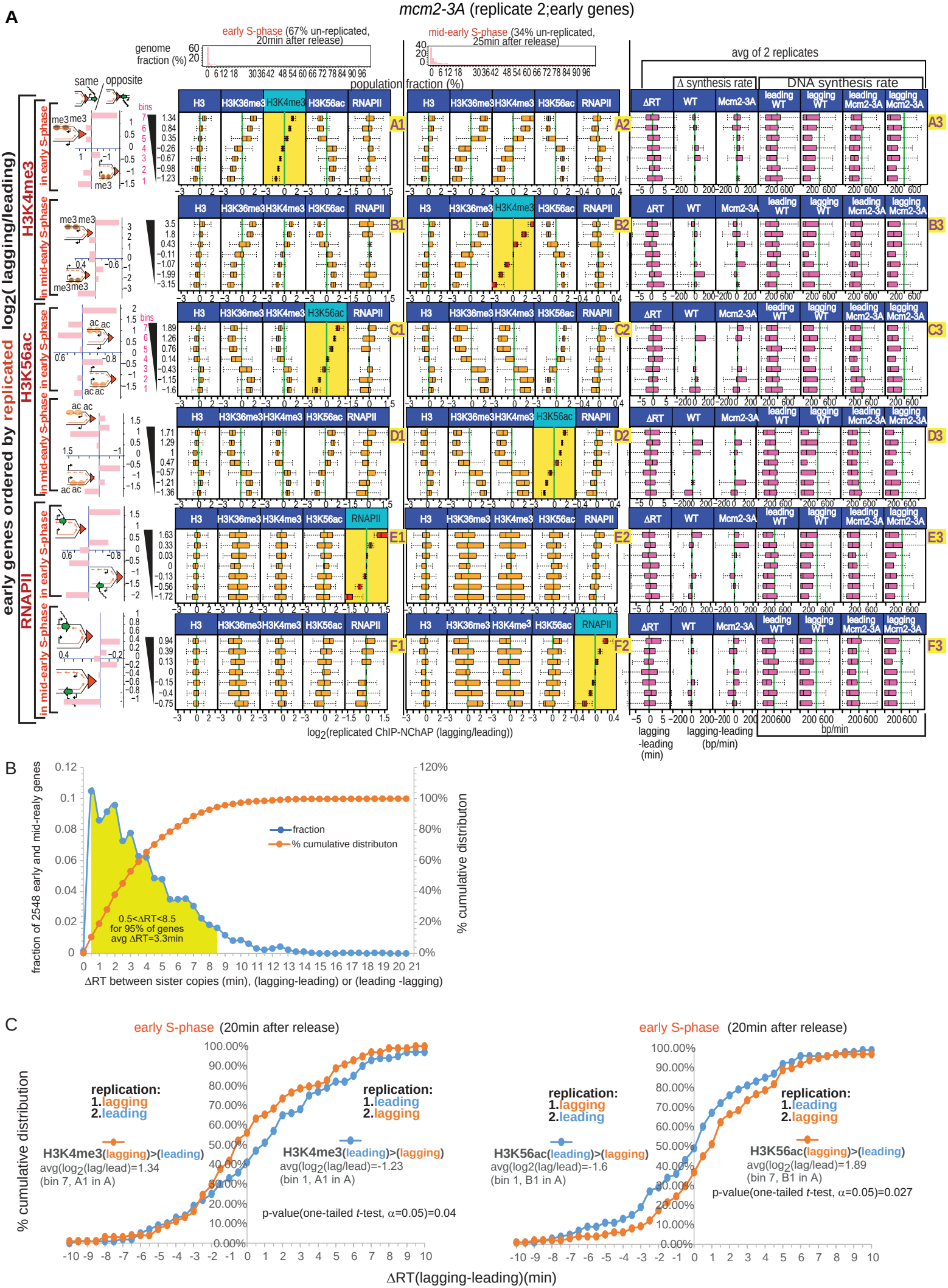

Figure S9:Chromatin maturation in *mcm2-3A* cells, replicate 2. (related to Figures 6 and S8)

Supplemental Fig S9: Chromatin maturation in *mcm2-3A* cells, replicate 2 (related to Figures 6 and Supplemental Fig S8): A. Box plot distribution of H3, H3K4me3, H3K36me3, H3K56ac and RNAPII on the lagging and leading strands for *mcm2-3A* biological replicate 2. The layout is the same as in Figure 6A and Supplemental Figure S8A. **B.** Distribution of the differences in replication timing between sister gene copies (ΔRT, lagging-leading and leading-lagging) in *mcm2-3A* cells for all early and mid-early genes. The yellow surface shows 95% of early and mid-early genes whose ΔRT is between 0.5 and 8.5 min. avg ΔRT=3.5min is the average of the whole gene population represented in the plot (n=2548).**C.** Cumulative distribution of differences in Replication Timing between the lagging and the leading sister gene copy (ΔRT) for the top (bin 7, orange) and bottom (bin 1, blue) gene bins from A, field A3 (ordered by H3K4me3 $\log_2$(lagging/leading) in early S-phase, left panel) and field C3 (ordered by H3K56ac $\log_2$(lagging/leading) in early S-phase, right panel).

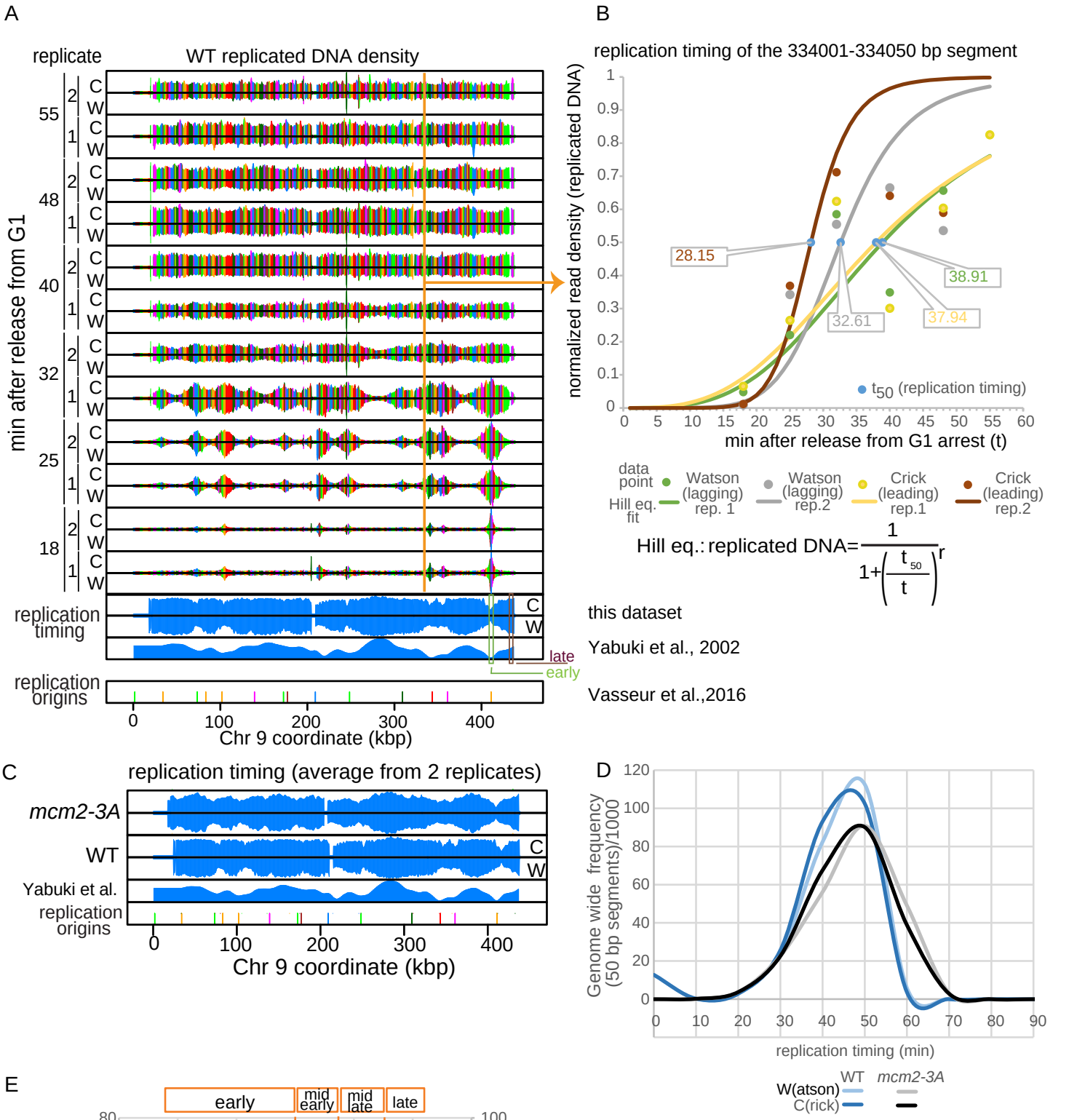

Figure S10: Calculations of replication timing and DNA synthesis rates per gene for WT and *mcm2-3A* strains.

Supplemental Fig S10: Calculations of replication timing per gene for WT and *mcm2-3A* strains (related to Figures 5 and 6). A. 400bp binned input normalized read density of replicated DNA (NChAP) for Chr 9, measured in two WT replicates from a time course after release from alpha factor G1 arrest. Genes are delimited by different colors. The Watson (W) and Crick(C) strands are analyzed separately. To calculate replication timing shown in the 3rd and 4th rows from the bottom reads from each time point were binned in 50bp segments and normalized by dividing each segment density with the highest density in the chromosome. The normalized densities were then smoothed with a 1600bp moving window average. Read densities for each 50bp segment were then plotted against time as shown in B. **B.** A curve described by the Hill equation was fitted to data points from the time course from A and replication timing was calculated from the Hill equation fit. **C.** Replication timing profiles of chr9 for Watson (W) and Crick (C) strands of WT and *mcm2-3A* strains. **D.** Replication timing distribution of all 50bp segments in the genome for WT and *mcm2-3A*. **E.** *mcm2-3A* replication timing versus WT replication timing for the Watson (W) strand (right, Y axis) and the Crick (C) strand (left, Y axis). All late replicating and a portion of mid-late replicating genes replicate ~10min later in the *mcm2-3A* mutant compared to WT.

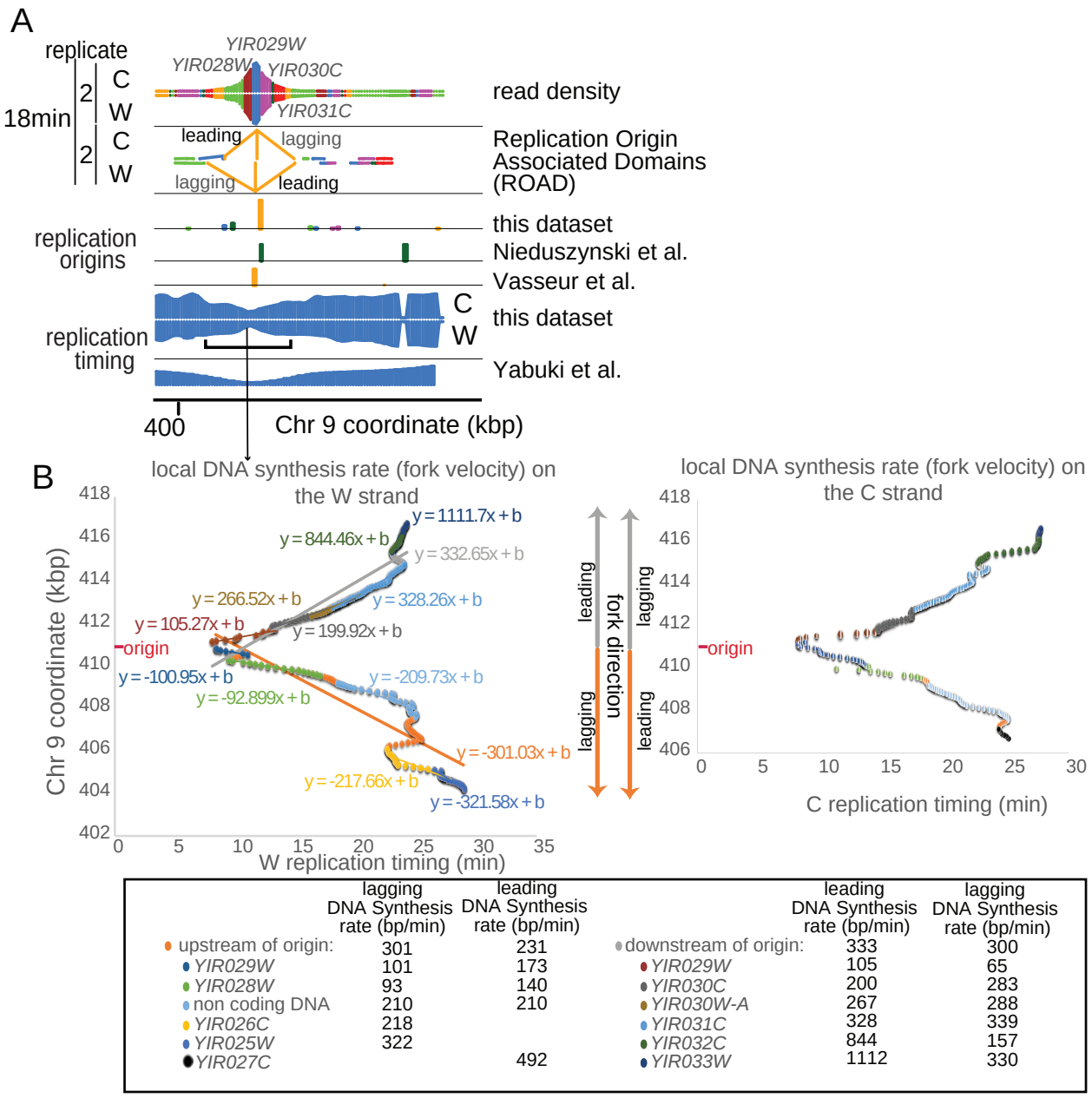

	lagging DNA Synthesis rate (bp/min)	leading DNA Synthesis rate (bp/min)		leading DNA Synthesis rate (bp/min)	lagging DNA Synthesis rate (bp/min)
upstream of origin:	301	231	downstream of origin:	333	300
YIR029W	101	173	*YIR029W*	105	65
YIR028W	93	140	*YIR030C*	200	283
non coding DNA	210	210	*YIR030W-A*	267	288
YIR026C	218		*YIR031C*	328	339
YIR025W	322		*YIR032C*	844	157
YIR027C		492	*YIR033W*	1112	330

Figure S11: Calculations of DNA synthesis rates per gene.

Supplemental Fig S11 (related to Figure 6): Calculations of DNA synthesis rates per gene. Replication timing values from Supplemental Fig S10 were used to calculate DNA synthesis rates of the Watson and Crick strands at every replicated gene from the 18min and 25min time points from Supplemental Fig S10A. **A.** First replication origins were determined from local peaks in the 18min et 25min time points. Second, genes that are replicated from any given origin were grouped into Replication Origin Associated Domains (ROADs) for either time point as illustrated for the 18min time point. ROADs are regions that have been replicated from the same origin. **B.**The average DNA synthesis rates of the Watson (W) (left) and Crick (C) (right) strands at each gene from every ROAD were calculated from the slope of the linear fit of the gene coordinates in bp versus replication timing as shown in the graphs. Synthesis rates of lagging strand gene copies are derived from slopes from the Watson strand upstream of origins and the Crick strand downstream of origins. Conversely leading strand synthesis rates come from Crick strands upstream and Watson strands downstream of origins. Synthesis rates for genes associated with the ROAD from A are summarized in the table below the graphs.

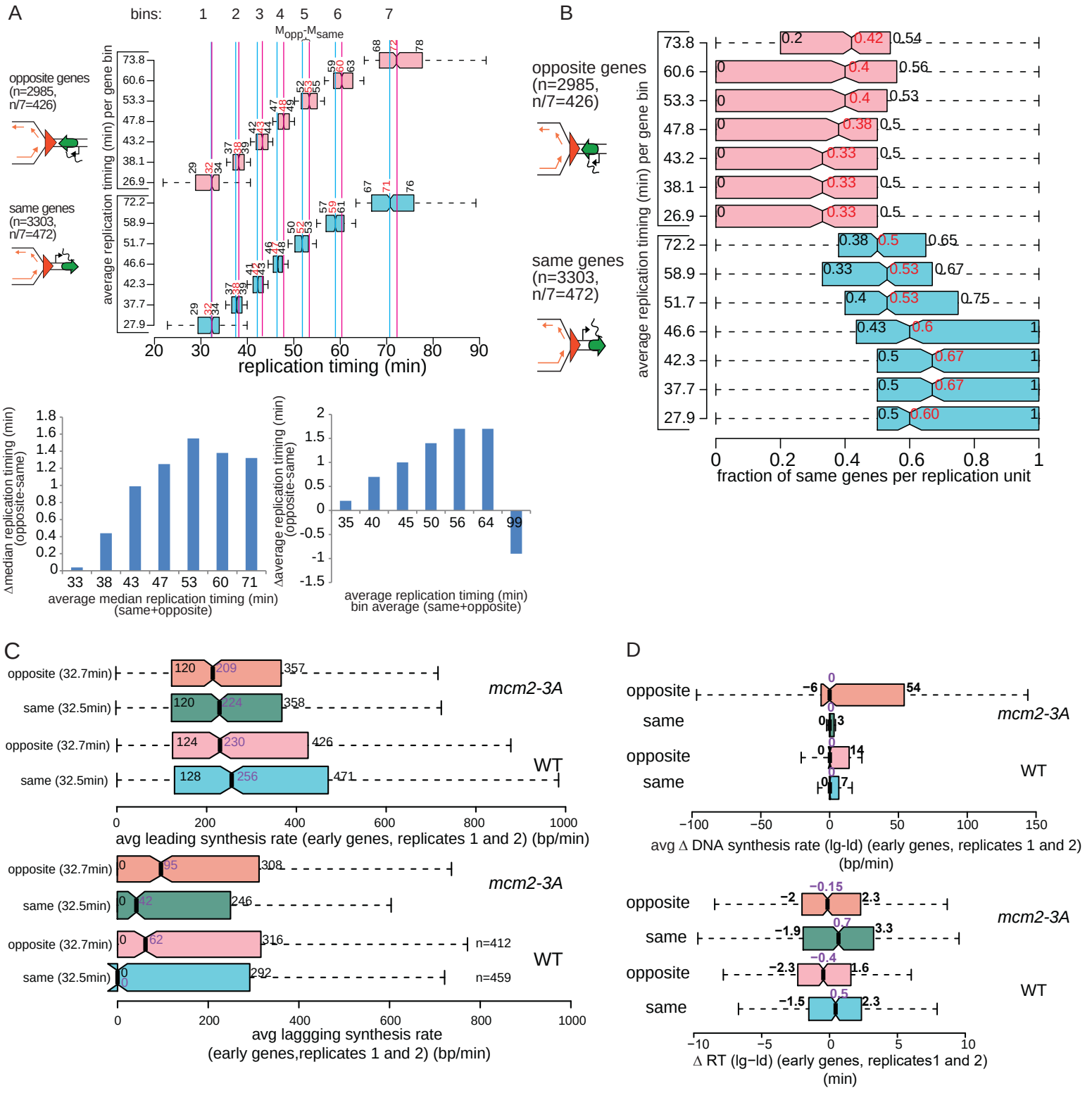

Figure S12: Differences in replication timing and DNA synthesis rates between "same" and "opposite" genes.

Supplemental Fig S12: Differences in replication timing and DNA synthesis rates between "same" and "opposite" genes (related to Figures 5, 6 and 7). A. Replication timing differences of "same" and "opposite" genes. 6288 yeast genes were divided into "same" (3303 genes) and "opposite" (2985 genes) orientation genes, sorted by replication timing (Vasseur et al., 2016) and then divided into seven equal bins each (numbered above the plot, 426 and 472 genes per bin for opposite and same genes, respectively, top panel). Top panel: box plot distributions of replication timing were determined for each bin. Second and third quartile medians (M) are shown in black above each box. Medians for the entire distribution are shown in red. M_{opp} - M_{same} (marked on bin 5) is the difference in median replication timing between "opposite" (pink) and "same" (blue) genes. Bottom panel: Bar graphs of the differences in median (left) or average replication timing (right) between opposite and same genes for each bin. The x axis shows the average of median (left) or average replication timing (right) of same and opposite gene bins (1 to 7). **B.** Genic orientation bias within replication units. The ensemble of all the genes that replicated from the same closest replication origin and are on the same side of that origin (upstream or downstream) define each replication unit or ROAD (Replication Origin Associated Domain) as in Supplemental Figure S11A. To determine whether any given gene is more likely to be surrounded by genes of the same genic orientation within each ROAD, the fraction of "same" orientation genes was calculated for each ROAD. We then determined box plot distributions of "same" gene fractions from ROADS assigned to genes from each replication timing bin defined in A. Second and third quartile medians are shown in black and medians for the entire distribution are shown in red. **C.** Box plot distribution of lagging (bottom) and leading (top) strand DNA synthesis rates for "same" (n=459) and" opposite" (n=412) early replicating genes in WT and *mcm2-3A* mutants. The average replication timing for the gene group (from Vasseur et al., 2016) is in parenthesis on the left. Synthesis rates are an average of two replicates (replicates 1 from Figures 5 and 6 and replicates 2 from Supplemental Figs S7 and S9). The median values are shown in purple and the 2nd and 3rd quartiles in black. **D.** Top: Box plot distribution of the difference in DNA synthesis rates between lagging and leading (lg-ld) copies of "same" and "opposite" early genes as in C. Bottom: Distribution of the differences between replication timing (ΔRT) of lagging and leading strands from the same group of genes as in C.

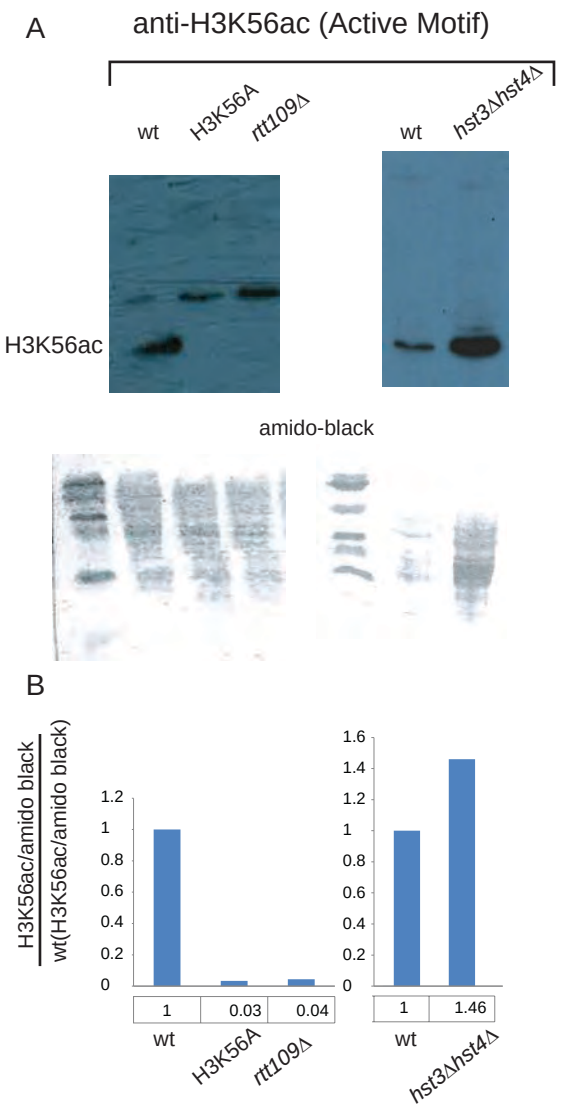

Figure S13: Specificity test for the anti H3K56ac antibody (Active Motif).

Supplemental Fig S13: Specificity test for the anti H3K56ac antibody (Active Motif). A. Western blots with midlog cell extracts from indicated strains. WT: W303 (MATa ade2-1 his3-11,15 leu2-3,112 trp1-1 ura3-1 can1-100); *rtt109Δ*: strain RZ72; H3K56A: AC33; *hst3Δhst4Δ*: AC29; Genotypes are listed in Table S3. The bottom panel shows the amido-black staining of the gels in the top panel. **B.** Quantification of western blots in A. H3K56ac background corrected band intensities were divided by the intensity of the corresponding lane stained with amido black. Band intensities were determined using the Gel Analyzer software (GelAnalyzer.com, Istvan Lazar). The background signal was determined with the rolling ball method (radius= 50).

.